Analysis of transient electron energy in a micro dielectric barrier discharge for a high performance plasma display panel

Giichiro Uchida,[1,a)] Satoshi Uchida,[2] Hiroshi Kajiyama,[1] and Tsutae Shinoda[1]
[1]*Graduate School of Advanced Science of Matter, Hiroshima University, Higashi-Hiroshima 739-8530, Japan*
[2]*Graduate School of Science and Engineering, Tokyo Metropolitan University, Hachiouji 192-0397, Japan*

(Received 15 October 2009; accepted 14 December 2009; published online 25 January 2010)

We present here analysis of electron energy of a micro dielectric barrier discharge (micro-DBD) for alternating-current plasma display panel (ac-PDP) with Ne/Xe gas mixture by using the optical emission spectroscopy (OES). The OES method is quite useful to evaluate a variety of electron energy in a high pressure DBD ignited in a PDP small cell. Experiment shows that the ratio of Ne emission intensity (I_{Ne}) relative to Xe emission intensity (I_{Xe}) drastically decreases with time. This temporal profile is well consistent with dynamic behavior of electron temperature in a micro-DBD, calculated in one-dimensional fluid model. I_{Ne}/I_{Xe} also decreases with an increase in Xe gas pressure and a decrease in applied voltage especially in the initial stage of discharge, and these reflect the basic features of electron temperature in a micro-DBD. The influences of plasma parameters such as electron temperature on luminous efficacy are also theoretically analyzed using one-dimensional fluid model. The low electron temperature, which is attained at high Xe gas pressure, realizes the efficient Xe excitation for vacuum ultraviolet radiation. The high Xe-pressure condition also induces the rapid growth of discharge and consequent high plasma density, resulting in high electron heating efficiency. © *2010 American Institute of Physics*. [doi:10.1063/1.3291123]

I. INTRODUCTION

A micro dielectric barrier discharge (micro-DBD) is presently an interesting topic in atmospheric micro-plasma physics and engineering. Plasma display panel (PDP) utilizing the vacuum ultraviolet (VUV) emission from Ne/Xe gas discharge is a major application of a micro-DBD.[1,2] The discharge efficiency of PDP producing VUV light is still much lower than other plasma application utilizing VUV radiation from discharge such as fluorescent lamps and Xe lamps. Therefore, it is an essential issue to understand and control complicated plasma phenomena in ac-PDP in order to develop high performance ac-PDP. High Xe concentration of discharge gas is recently becoming one of the most promising approaches to improve the luminous efficiency,[3–5] and this effect is generally explained by the contribution of Xe excimer molecules to the VUV radiation. However, the increase in Xe gas pressure varies not only the reaction chemistry related to the VUV radiation but also fundamental plasma parameters at the same time. Particularly, electron energy is quite important for luminous efficacy of ac-PDP because an essential process for generating large VUV radiation is to efficiently excite Xe neutral atom by electron with appropriate energy. Therefore, understanding the basic features of electron energy in ac-PDP is quite important for designing a cell structure and driving waveform to achieve high performance PDP. Laser Tomson Scattering diagnostic has been applied to a measurement of the plasma parameters in a micro-DBD for PDP by Noguchi *et al.*,[6] and electron temperature and plasma density are reported to be 3–4 eV and the order of 10^{13} cm^{-3}, respectively. But, the diagnostic requires the special panel through which laser beam can pass, and is difficult to be applied to the measurement of ac-PDP like commercial products. On the other hand, the optical emission spectroscopy (OES),[7–9] in which only emission spectrum is captured through the transparent front glass of ac-PDP, is quite useful to roughly estimate electron energy of a small and transient discharge in ac-PDP. There have been many works on the spectroscopy of emission from ac-PDP and basic knowledge of a microdischarge in a ac-PDP cell has been experimentally studied for the past decade.[3,10–17] The main purpose of this paper, on the other hand, is to discuss the VUV radiation efficiency in the view of fundamental plasma parameters and a focus is on the analysis of the dynamic behavior of electron energy. Our experiment and simulation analysis clearly show that electron energy is relatively high in the initial stage of discharge, and drastically decreases with time. The electron energy is found to be sensitive to Xe gas pressure and applied voltage and considerably affects the VUV radiation efficiency. First, we report the experiment on high time-resolved emission spectra. Then, we present the simulation analysis of ac-PDP related to plasma parameters.

II. EXPERIMENTS

A 4 in. test PDP is used to investigate the dynamics of electron energy in a PDP small cell. Here, the electrodes of the front panel are a standard stripe with 180 μm in width, and interelectrode distance between the *X* and *Y* electrode is 80 μm as shown schematically in Fig. 1. The electrodes are covered by the dielectric layer of 30 μm and then a 500 nm thick protective layer. A micro-DBD in each cell is ignited by applying the 15 kHz square sustaining voltage (V_s) to the

[a)]Electronic mail: giichiro@hiroshima-u.ac.jp.

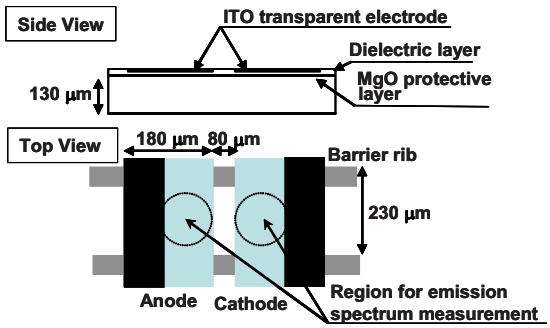

FIG. 1. (Color online) A cell dimension of ac-PDP for the OES.

pair sustaining electrodes. The gas used for DBD production is a mixture of Ne and Xe in the pressure range from 100 to 700 Torr, and the Xe partial concentration (C_{Xe}) is varied from 4% to 20%. In order to analyze temporal behavior of electron energy with the OES diagnostic, the high time-resolved emission spectra are measured by spectral analyzer with microchannel plate (MCP) system that amplifies the detected signal, where the MCP system is gated with 20 ns. A microscope is also set above the panel for observing emission spectra from cathode and anode region in a cell, as shown in Fig. 1.

Figure 2 shows a typical temporal evolution of emission spectra from ac-PDP for Ne/Xe gas pressure=220 Torr and Xe concentration (C_{Xe})=4%. We can detect various emissions in the wavelength range from 540.0 to 743.8 nm from Ne atom and from 788.7 to 1083.8 nm for Xe atom, respectively, where the strongest emission lines are Ne:585.2 nm and Xe:823.1 nm. Generally, for all rare gases, the first excited state consists of four levels as shown in Fig. 3. In Paschen's notation, two levels $1s_3$ and $1s_5$ are metastable state, and the other two lowing levels $1s_2$ and $1s_4$ are resonance state. The next excited configuration contains ten levels which are denoted as $2p_1$ through $2p_{10}$. The various lines are emitted as electrons decay from the Paschen $2p$ level to

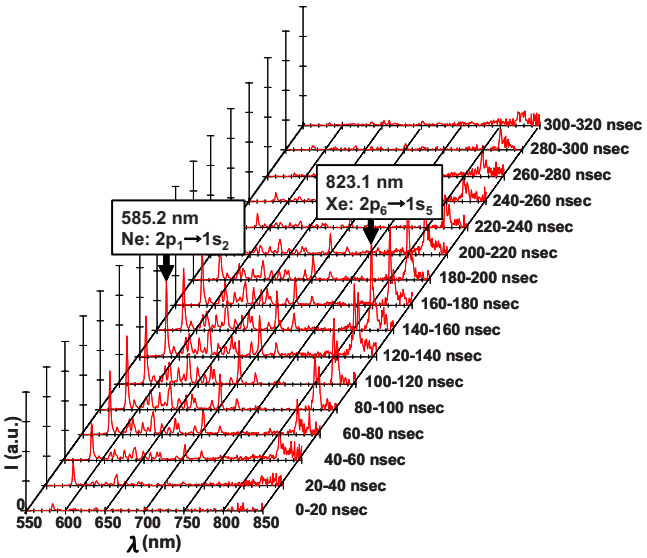

FIG. 2. (Color online) Temporal evolution of optical emission spectra from ac-PDP for Ne/Xe pressure ($P_{Ne/Xe}$)=220 Torr and Xe concentrations (C_{Xe})=4.0%.

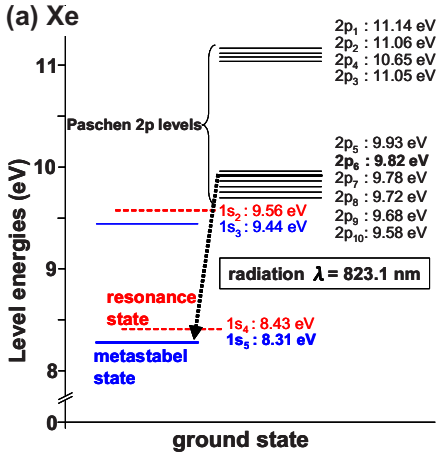

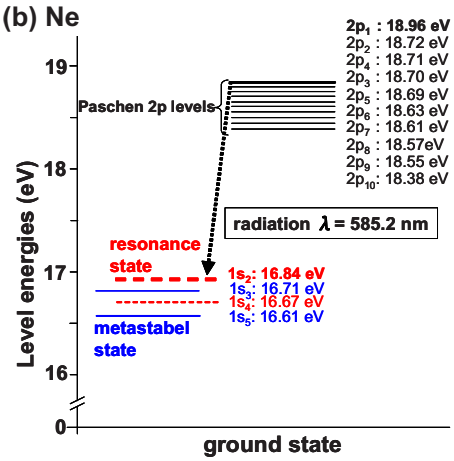

FIG. 3. (Color online) Energy levels of (a) Ne and (b) Xe atoms.

one of the four $1s$ states, where Xe:823.1 nm from $2p_6$ to $1s_5$, and Ne:585.2 nm from $2p_1$ to $1s_2$. Figure 4(a) shows the cross sections for electron-impact excitation from ground state to $2p_6$ and $2p_1$ in Xe and Ne atoms, respectively.[18,19] The cross sections are found to be very sensitive to the impinging electron energy (E_e), and Ne and Xe atoms can be

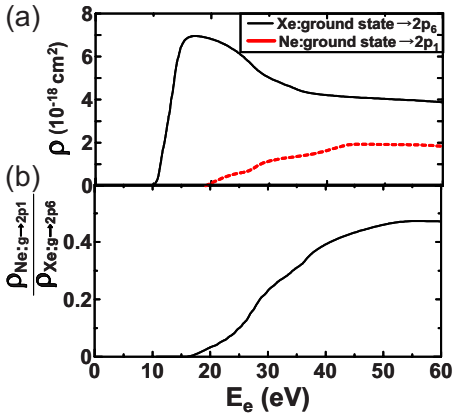

FIG. 4. (Color online) (a) The cross sections for electron-impact excitation from ground state to $2p_6$ and $2p_1$ in Xe and Ne atoms, respectively. These reactions are related to the emissions of Xe:823.1 nm and Ne:585.2 nm. (b) The ratio of the Ne cross-section to the Xe cross-section as a function of imping electron energy (E_e).

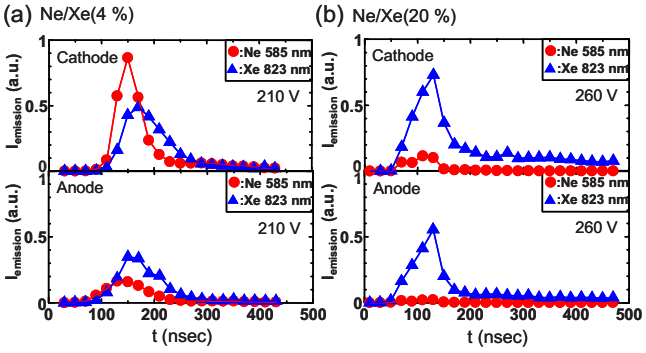

FIG. 5. (Color online) Ne:585 nm and Xe:823 nm emission intensities for ac-PDP with Xe concentrations (C_{Xe}) of (a) 4% and (b) 20%, and Ne/Xe pressure ($P_{Ne/Xe}$)=500 Torr. Emission intensities are observed at electrical breakdown voltage of each panel.

excited by electrons with above 18.71 and 9.81 eV, respectively. Figure 4(b) also shows the ratio of the Ne cross-sections to the Xe cross-section as a function of E_e. The probability of Ne-emission relative to Xe-emission increases linearly with E_e up to about 40 eV, and this indicates that the variety of imping electron energy can be roughly estimated by the Ne-to-Xe emission ratio observed.[7,8,11]

Figure 5 shows temporal behaviors of spectrum intensities of Ne and Xe emission with 585.2 and 823.1 nm in wavelength ($I_{Xe(582\ nm)}$ and $I_{Ne(823\ nm)}$), where (a) and (b) are results for C_{Xe}=4 and 20%, respectively. The emission intensities are measured at the electrical breakdown voltage 210 and 260 V for C_{Xe}=4 and 20%, respectively. For C_{Xe}=4%, $I_{Ne(585\ nm)}$ is very large in cathode region. As C_{Xe} is varied from 4 to 20%, $I_{Ne(585\ nm)}$ drastically decreases by a factor of 10 both in the cathode and anode regions, while $I_{Xe(823\ nm)}$ becomes only 1.5 times larger than that of C_{Xe}=4%.

After this, we investigate the spectrum-intensity ratio of Ne:585.2 nm and Xe:823.1 nm ($I_{Ne(585\ nm)}/I_{Xe(823\ nm)}$) for various gas conditions ($P_{Ne/Xe}$). In Fig. 6, the temporal evolutions of $I_{Ne(585\ nm)}/I_{Xe(823\ nm)}$ are plotted as a parameter of an applied voltage (V_s), for (a) C_{Xe}=4% and $P_{Ne/Xe}$ =100 Torr, (b) C_{Xe}=4% and $P_{Ne/Xe}$=500 Torr, and (c) C_{Xe}=20% and $P_{Ne/Xe}$=500 Torr, which correspond to Xe partial pressure (P_{Xe}) of (a) 4 Torr, (b) 20 Torr, and (c) 100 Torr, respectively. Here, relative spectrum intensity is normalized by neutral Ne and Xe gas density (n_{Ne} and n_{Xe}), because $I_{Ne(585\ nm)}$ and $I_{Xe(823\ nm)}$ are simply linear to n_{Ne} and n_{Xe}, respectively. The peak time of $I_{Ne(585\ nm)}$ is marked by arrows, where the peak $I_{Ne(585\ nm)}$ is observed at the almost same time with a discharge current peak. As can be seen in Fig. 6, $I_{Ne(585\ nm)}/I_{Xe(823\ nm)}$ is relatively large in the initial period of discharge, and drastically decreases with time both in the cathode (Ca) and anode (An) areas for all gas conditions. $I_{Ne(585\ nm)}/I_{Xe(823\ nm)}$ also decreases with increasing Xe partial pressure (P_{Xe}) especially in the initial stage of discharge. The result clearly demonstrates that for higher P_{Xe}, a micro-DBD is ignited by lower energy electrons, even though higher voltage is applied to sustaining electrodes. Figure 7 summarizes $I_{Ne(585\ nm)}/I_{Xe(823\ nm)}$ as a parameter of (a) $P_{Ne/Xe}$ and (b) C_{Xe}, where the values are compared at the time of a peak $I_{Ne(585\ nm)}$ marked

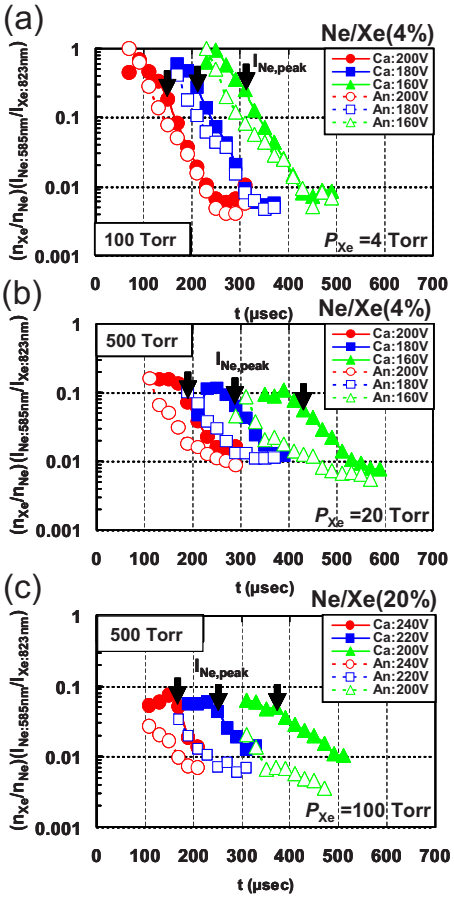

FIG. 6. (Color online) Temporal behaviors of relative spectrum intensities of Ne:585.2 nm and Xe:823.1 nm emission, where the relative emission intensities are normalized by neutral gas densities in order to compare the emission ratios under various gas conditions. (a) C_{Xe}=4% and $P_{Ne/Xe}$ =100 Torr, (b) C_{Xe}=4% and $P_{Ne/Xe}$=500 Torr, and (c) C_{Xe}=20% and $P_{Ne/Xe}$=500 Torr, which corresponds to the Xe partial pressure (P_{Xe}) of (a) 4 Torr, (b) 20 Torr, and (c) 100 Torr, respectively.

by arrows in Fig. 6. $I_{Ne(585\ nm)}/I_{Xe(823\ nm)}$ decreases with an increase in $P_{Ne/Xe}$ and C_{Xe}, and slightly decreases as an applied voltage (V_s) decreases. As a result, the minimum $I_{Ne(585\ nm)}/I_{Xe(823\ nm)}$, which implies the lowest electron energy, is obtained at higher $P_{Ne/Xe}$ and C_{Xe} and lower V_s, as denoted by triangle in Fig. 7. From these results we can conclude that the electron energy in ac-PDP is sensitive to Xe gas condition and applied voltage especially in the initial period of discharge.

III. SIMULATION ANALYSIS

Various groups have already performed simulation analysis of ac-PDP.[20–27] On our simulation, we focus on the analysis of the detailed relationship between plasma parameters and luminous efficacy of PDP. First, electron energy is theoretically analyzed using one-dimensional fluid model. Here, the reaction process considered in the simulation are listed in Ref. 28. Figure 8 shows dynamic behavior of a DBD-structure, where (a), (b), and (c) are space profiles of potential (V_{space}), electron density (n_e), and electron temperature (T_e), respectively, at Ne/Xe(10%)=67 kPa. Here, cathode and anode electrodes are set at 0 and 80 μm, respectively. V_{space} increases linearly from cathode toward anode

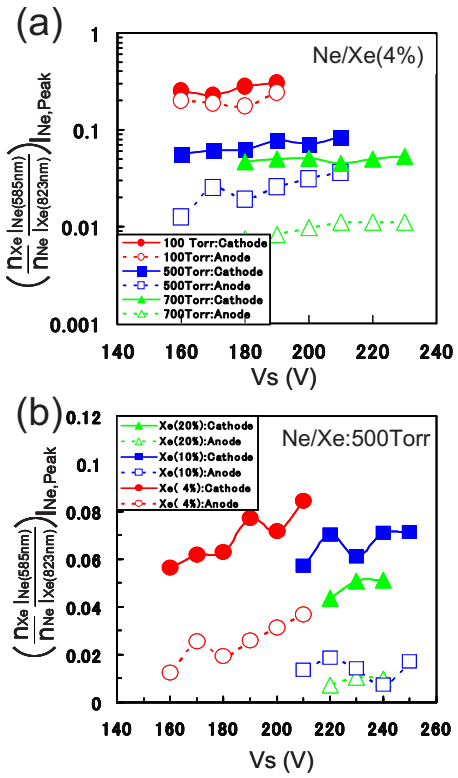

FIG. 7. (Color online) Sustaining voltage (V_s) dependence of relative spectrum intensity of Ne:585.2 nm and Xe:823.1 nm as a parameter of (a) Ne/Xe gas pressure ($P_{Ne/Xe}$) and (b) Xe concentration (C_{Xe}), where the relative emission intensity is normalized by neutral gas densities. The values are compared at the time of a peak $I_{Ne(585\ nm)}$ marked by arrows in Fig. 6.

before the electrical breakdown. Once the breakdown occurs at about 100 ns, electron density (n_e) gradually increases with time, being accompanied with the movement of a position of a peak density ($n_{e,peak}$) towards cathode side, as de-

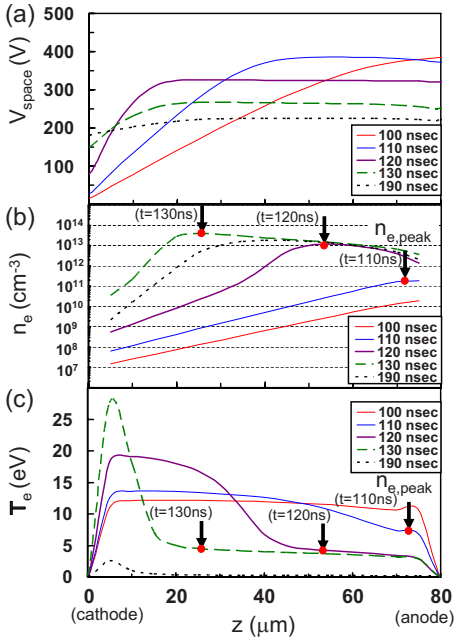

FIG. 8. (Color online) Spatiotemporal evolution of a micro-DBD, where (a), (b), and (c) are potential (V_{space}), electron density (n_e), and electron temperature (T_e), respectively, at Ne/Xe(10%)=67 kPa.

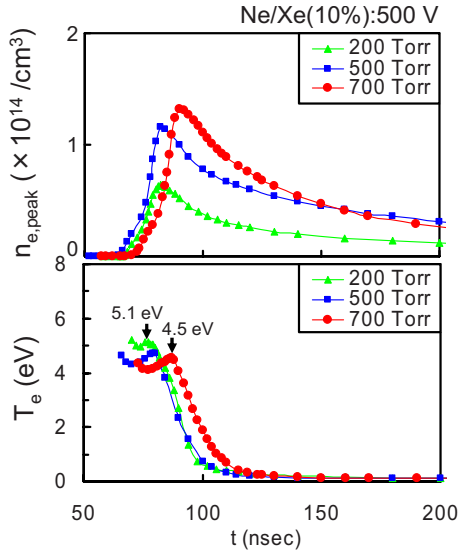

FIG. 9. (Color online) Temporal behavior of a peak electron density ($n_{e,peak}$) and electron temperature (T_e) as a parameter of Ne/Xe gas pressure. Sustaining voltage (V_s)=500 V. Here, T_e is evaluated at a position where $n_{e,peak}$ has a maximum.

noted by arrows in Fig. 8(b). An increase in plasma density induces the distortion of V_{space}, and eventually the ion sheath with strong electric field is formed in front of the cathode electrode at 120 ns (purple line), as found in Fig. 8(a). Then, the ion-sheath structure gradually collapses due to the accumulation of charged particle on dielectric layer covered over the cathode electrode (t=120–190 ns). As can be seen at 130 ns (green line) in Fig. 8(c), electron temperature is quite high in the ion sheath region due to the acceleration of electron by strong electric field, and drastically decreases due to the dissipation of energy by ionization and excitation via collisions. Then, a peak density $n_{e,peak}$ is observed at 25 μm, where electron temperature is about 5 eV. Figures 9 and 10 show temporal behaviors of $n_{e,peak}$ and T_e as a parameter of

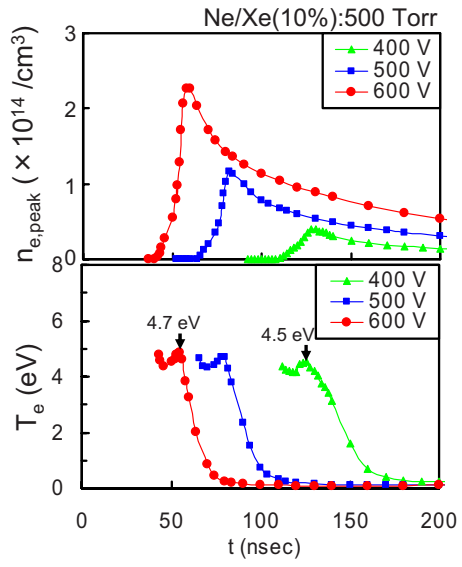

FIG. 10. (Color online) Temporal behavior of a peak electron density ($n_{e,peak}$) and electron temperature (T_e) as a parameter of sustaining voltage (V_s). Ne/Xe (10%) gas pressure=500 Torr. Here, T_e is evaluated at a position where n_e has a maximum.

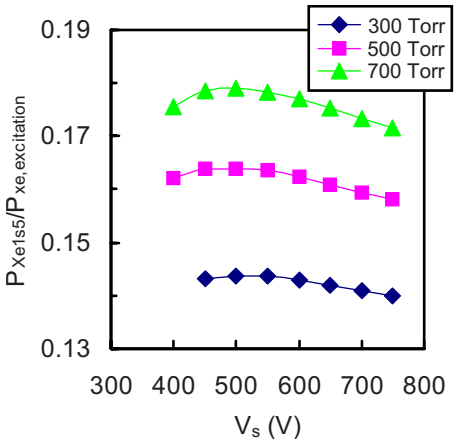

FIG. 11. (Color online) The ratio of electron impact excitation directly from ground state to Xe lowest level $1s_5$ (P_{Xe1s_5}) relative to the total excitations in Xe atom ($P_{Xe,excitation}$), as a function applied voltage (V_s) with gas pressure as a parameter.

gas pressure and applied voltage (V_s), respectively. Here, T_e is evaluated at a position where $n_{e,peak}$ is observed. T_e is relatively high in the initial stage of discharge, and drastically decreases with time. It is worth noting that the temporal behavior of T_e is well consistent with $I_{Ne(585\ nm)}/I_{Xe(823\ nm)}$ observed in experiment (see Fig. 6). T_e also decreases with an increase in gas pressure and a decrease in V_s, as is also consistent with the variety of I_{Ne}/I_{Xe} as shown in Fig. 7. Our simulation theoretically demonstrates the dynamic behavior of electron energy in a micro-DBD.

Then, we analyze the influence of plasma parameters such as T_e and n_e on luminous efficacy of ac-PDP. Figure 11 shows the ratio of electron impact excitation directly from ground state to Xe lowest level $1s_5$(P_{Xe1s_5}) relative to the total excitations in Xe atom ($P_{Xe,excitation}$). The lower levels such as $1s_5$ and $1s_4$ play important role as precursors of VUV radiation of 147 and 172 nm. Therefore, the direct-excitations to these lower levels are considered to be most efficient reaction processes related to the VUV radiation. $P_{Xe1s_5}/P_{Xe,excitation}$ is observed to increase with increasing gas pressure and decreasing V_s. The result indicates that lower electron energy, which can be realized at high gas pressure and low V_s, is advantageous for the direct-excitation processes to lowing state levels, resulting in efficient VUV radiation.

Figure 12 shows temporal evolutions of $n_{e,peak}$ and electron heating efficiency (η_e), at (1) 500 V and 200 Torr, (2) 500 V and 500 Torr, and (3) 600 V and 500 Torr. Here, η_e is defined as the ratio of energy to be transferred to electrons from the electrical input energy.[22] Higher gas pressure and V_s lead to the rapid growth of discharge and consequent high plasma density, and higher η_e is attained at that time especially in initial stage of discharge. These results confirm that more frequent ionizations in initial period of discharge leads to higher η_e. It must be emphasized that in the latter period of pulse-discharge, η_e becomes very low, due to the significant dissipation of the input power to many ions concentrated in the cathode sheath, namely, the dominating ion heating loss in the ion sheath.[14,15] Figure 13 summarizes the

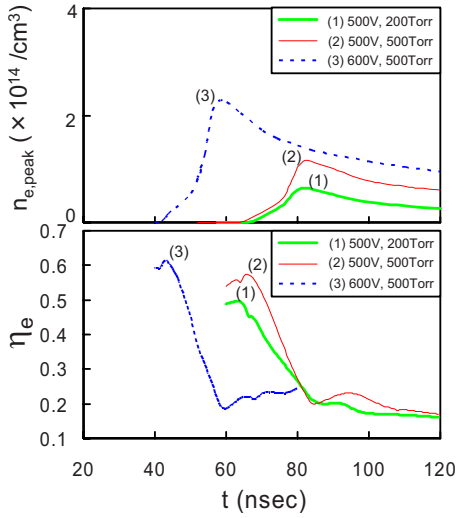

FIG. 12. (Color online) Temporal behaviors of an electron peak density ($n_{e,peak}$) and electron heating efficiency (η_e), which is given as the ratio of the electrical input power to be transferred to the energy of the electron at (1) 500 V and 200 Torr, (2) 500 V and 500 Torr, and (3) 600 V and 500 Torr.

V_s dependence of η_e as a parameter of gas pressure. η_e increases with gas pressure and V_s, and this considerably contributes to high luminous efficacy of PDP.

IV. DISCUSSION AND CONCLUSION

We have described the time-resolved measurements of $I_{Ne(585\ nm)}/I_{Xe(823\ nm)}$. The temporal feature of $I_{Ne(585\ nm)}/I_{Xe(823\ nm)}$ is very similar to the behavior of calculated T_e, and this clearly indicates that the observation of I_{Ne}/I_{Xe} is quite effective to roughly estimate the variety of T_e in a micro-DBD. T_e is relatively high in the initial stage of discharge, being followed by an abrupt decrease. In our simulation, T_e keeps around 5 eV at a period from discharge ignition to the completion of sheath formation and then drastically decreases with the collapse of sheath structure. These results show that the dynamic behavior of electron energy is closely related to the transient potential structure in a micro-DBD. $I_{Ne(585\ nm)}/I_{Xe(823\ nm)}$ observed is also sensitive to the Xe gas pressure and applied voltage (V_s) especially in initial stage of discharge. For higher Xe contents, it is difficult to accelerate electrons by electric field because of the large col-

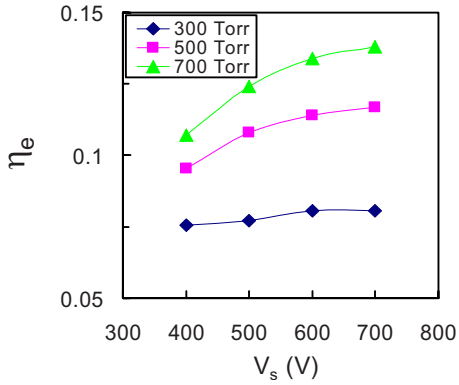

FIG. 13. (Color online) The sustaining voltage (V_s) dependence of electron heating efficiency (η_e) as a parameter of Ne/Xe(10%) gas pressure.

lisional cross section of Xe atom, which is responsible for lower T_e observed at higher Xe partial pressure. V_s, on the other hand, directly modifies the electric field strength, and affects T_e especially in the early period of discharge.

Our calculation clearly shows a desirable plasma condition for high performance PDP. Low T_e induces the efficient Xe-excitation process related to VUV radiation, and also the rapid growth of discharge leads to high electron heating efficiency (η_e). A micro-DBD at high Xe pressures realizes these plasma conditions, and is appropriate for high performance ac-PDP also in the view of plasma condition.

In conclusion, our experiment clearly demonstrates a dynamic behavior of electron energy in a ac-PDP small cell. Electron energy drastically decreases with time and also quite sensitive to Xe gas pressure and applied voltage especially in initial stage of discharge. Basic plasma parameters such as electron energy considerably influence luminous efficacy of ac-PDP and the time- and space-resolved OES is quite useful to investigate transient electron energy in ac-PDP.

ACKNOWLEDGMENTS

This work was partly supported by New Energy Development Organization (NEDO) and Advanced PDP Development Center Corp. (APDC). We would like to thank ULVAC. Inc. for cooperation of PDP experiment system. G.U. acknowledges stimulation conversation with T. Akiyama.

[1]T. Shinoda, M. Wakitani, T. Nanto, N. Awaji, and S. Kanagu, IEEE Trans. Electron Devices **47**, 77 (2000).
[2]J. P. Boeuf, J. Phys. D **36**, R53 (2003).
[3]T. Yoshioka, L. Tessier, A. Okigawa, and K. Toki, J. Soc. Inf. Disp. **8** 203 (2000).
[4]G. Oversluizen, S. de Zwart, S. van Heusden, and T. Dekker, J. Soc. Inf. Disp. **8**, 197 (2000).
[5]M. F. Gillies and G. Oversluizen, J. Appl. Phys. **91**, 6315 (2002).
[6]Y. Noguchi, A. Matsuoka, K. Uchino, and K. Muraoka, J. Appl. Phys. **91**, 613 (2002).
[7]M. V. Malyshev and V. M. Donnelly, J. Vac. Sci. Technol. A **15**, 550 (1997).
[8]M. V. Malyshev and V. M. Donnelly, Phys. Rev. E **60**, 6016 (1999).
[9]G. F. Karabadzhak, Y. C. Chiu, and R. A. Dressler, J. Appl. Phys. **99**, 113305 (2006).
[10]G. Oversluizen, M. Klein, S. de Zwart, S. van Heusden, and T. Dekker, Appl. Phys. Lett. **77**, 948 (2000).
[11]K. Suzuki, Y. Kawanami, S. Ho, N. Uemura, Y. Yajima, N. Kouchi, and Y. Hatano, J. Appl. Phys. **88**, 5605 (2000).
[12]G. Oversluizen, M. Klein, S. de Zwart, S. van Heusden, and T. Dekker, J. Appl. Phys. **91**, 2403 (2002).
[13]K. Tachibana, K. Mizokami, N. Kosugi, and T. Sakai, IEEE Trans. Plasma Sci. **31**, 68 (2003).
[14]G. Oversluizen and T. Dekker, J. Soc. Inf. Disp. **13**, 889 (2005).
[15]G. Oversluizen and T. Dekker, IEEE Trans. Plasma Sci. **34**, 305 (2006).
[16]G. Oversluizen, K. Itoh, T. Shiga, and S. Mikoshiba, J. Appl. Phys. **104**, 033303 (2008).
[17]T. S. Cho, G. H. Chung, and J. W. Jung, Appl. Phys. Lett. **92**, 221506 (2008).
[18]J. T. Fons and C. C. Lin, Phys. Rev. A **58**, 4603 (1998).
[19]J. E. Chilton, M. D. Stewart, Jr., and C. C. Lin, Phys. Rev. A **61**, 052708 (2000).
[20]J. Meunier, Ph. Belenguer, and J. P. Boeuf, J. Appl. Phys. **78**, 731(1995).
[21]S. Rauf and M. J. Kushner, J. Appl. Phys. **85**, 3460 (1999).
[22]G. J. Hagelaar, M. H. Klein, R. M. M. Snijkers, and G. M. W. Kroesen, J. Appl. Phys. **89**, 2033 (2001).
[23]H. C. Kim, M. S. Hur, S. S. Yand, S. W. Shin, and J. K. Lee, J. Appl. Phys. **91**, 9513 (2002).
[24]H. S. Bae, J. K. Kim, H. Y. Jung, J. K. Lim, and K. W. Whang, J. Appl. Phys. **95**, 30 (2004).
[25]W. J. Chung, B. J. Shin, T. J. Kim, H. S. Bae, J. H. Seo, and K.-W. Whang, IEEE Trans. Plasma Sci. **31**, 1038 (2003).
[26]H. S. Bae, J. K. Kim, H. Y. Jung, J. K. Lim, and K. W. Whang, J. Appl. Phys. **102**, 123308 (2007).
[27]D. Hayashi, G. Heusler, G. Hagelaar, and G. Kroesen, J. Appl. Phys. **95**, 1656 (2004).
[28]T. Kubota, S. Uchida, and F. Tochikubo, Jpn. J. Appl. Phys., Part 2 **48**, 046001 (2009).